3790 *Chem. Mater.* **2010,** *22,* 3790–3797
DOI:10.1021/cm100932j

CHEMISTRY OF MATERIALS
Article

Functional Composite Membranes Based on Mesoporous Silica Spheres in a Hierarchically Porous Matrix

Fan Li† and Andreas Stein*

Department of Chemistry, University of Minnesota, 207 Pleasant Street SE, Minneapolis, Minnesota 55455.
†Current address: DuPont Central Research & Development, Rt 141 and Henry Clay, Wilmington, DE 19803

Received April 2, 2010. Revised Manuscript Received May 3, 2010

We demonstrate a synthetic strategy toward functional, composite porous materials by incorporating functionalized porous silica spheres into a hierarchically porous silica matrix. Monodisperse mesoporous silica spheres decorated with organic probe molecules for visual Cd^{2+} ion detection were coated with a thin protecting poly(methyl methacrylate) (PMMA) layer to form core−shell particles. When these particles were redispersed in a mixture of a silica precursor, surfactant and hydrochloric acid, hierarchically structured composite films could be prepared by spin-coating and aging. The PMMA capsule protected the mesoporous silica spheres from being exposed to the silica precursor in the assembly step, which could have blocked the mesopores and/or reacted with the surface functional species. Once the polymer and surfactant components were removed by extraction while preserving the organic probe molecules within the silica spheres, composite porous structures were derived in which the mesoporous silica spheres were surrounded by a skeleton of another mesoporous silica phase. An observed color change of the film after exposure to analyte solutions with low concentrations of Cd^{2+} ions confirmed that the confined probe molecules remained active after the multiple processing steps and that they were accessible via the mesopores in the silica matrix surrounding the embedded spheres. By separating the sphere synthesis and functionalization steps from the film casting step, it is possible to choose different pore-forming surfactants during the syntheses of the spheres and the matrix, and in principle, to embed multiple sets of mesoporous spheres with different functional groups, whose syntheses may not be compatible with each other.

Introduction

With the proliferation of research on surfactant templating of ordered mesoporous silica,[1] much effort has been directed to applications of these materials in various areas, including sensing,[2] catalysis,[3] separation,[4] optics,[5] drug delivery,[6] and other uses. Besides the need for adjusting pore features to regulate mass transport or impose structural selectivity, the development of advanced applications often requires tailoring of the mesostructure to integrate it with other functional components. One representative example of an integrated, multifunctional system involves core−shell particles, which have been prepared by controlled growth of an oriented mesoporous layer around a magnetic core and have demonstrated potential as recyclable catalyst carriers in heterogeneous catalysis.[7,8] In addition, the formation of hierarchical systems requires coupling of mesopore formation with other templating methods or top-down lithographic techniques.[9,10]

Mesoporous silica with a great variety of functionalities can be prepared by modifying the mesopore interior. A particularly interesting direction involves the introduction of multiple types of functional groups. Although dual-functionality may be readily available if the intrinsic acidity of the silica surface is considered as one type of functionality,[11] under a more general standard it requires the placement of several distinct species inside the mesopores. Simultaneous or sequential functionalization with different reagents through co-condensation and post-grafting processes[12,13] are facile approaches, although they are not directly applicable to incompatible functional groups, for example, coexisting acidic and basic groups. In this case, controlled spatial distribution of

*To whom correspondence should be addressed. Tel.: (612) 624-1802. E-mail: a-stein@umn.edu.

(1) Wan, Y.; Zhao, D. *Chem. Rev.* **2007**, *107*, 2821–2860.
(2) Walcarius, A.; Collinson, M. M. *Annu. Rev. Anal. Chem.* **2009**, *2*, 121–143.
(3) Melero, J. A.; Van Grieken, R.; Morales, G. *Chem. Rev.* **2006**, *106*, 3790–3812.
(4) Dai, S. *Chem.—Eur. J.* **2001**, *7*, 763–768.
(5) Wirnsberger, G.; Stucky, G. D. *ChemPhysChem* **2000**, *1*, 90–92.
(6) Trewyn, B. G.; Slowing, I. I.; Giri, S.; Chen, H. T.; Lin, V. S. Y. *Acc. Chem. Res.* **2007**, *40*, 846–853.
(7) Deng, Y.; Qi, D.; Deng, C.; Zhang, X.; Zhao, D. *J. Am. Chem. Soc.* **2008**, *130*, 28–29.
(8) Ge, J.; Zhang, Q.; Zhang, T.; Yin, Y. *Angew. Chem., Int. Ed.* **2008**, *47*, 8924–8928.
(9) Li, F.; Wang, Z.; Ergang, N. S.; Fyfe, C. A.; Stein, A. *Langmuir* **2007**, *23*, 3996–4003.
(10) Kamperman, M.; Burns, A.; Weissgraeber, R.; van Vegten, N.; Warren, S. C.; Gruner, S. M.; Baiker, A.; Wiesner, U. *Nano Lett.* **2009**, *9*, 2756–2762.
(11) Sharma, K. K.; Anan, A.; Buckley, R. P.; Ouellette, W.; Asefa, T. *J. Am. Chem. Soc.* **2008**, *130*, 218–228.
(12) Asefa, T.; Kruk, M.; MacLachlan, M. J.; Coombs, N.; Grondey, H.; Jaroniec, M.; Ozin, G. A. *J. Am. Chem. Soc.* **2001**, *123*, 8520–8530.
(13) Lin, V. S. Y.; Lai, C. Y.; Huang, J.; Song, S. A.; Xu, S. *J. Am. Chem. Soc.* **2001**, *123*, 11510–11511.

Published on Web 05/24/2010

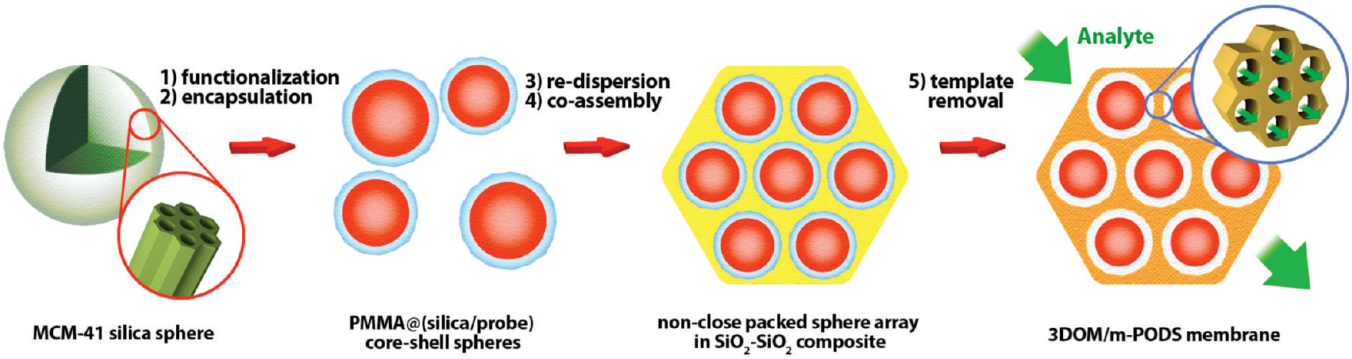

Figure 1. Schematic illustration of the fabrication of hierarchically porous nanocomposites for ion sensing and site isolation.

functional groups needs to be achieved to avoid their mutual destruction, and multiple-step procedures with carefully designed synthetic strategy become necessary.[14] Methods have been developed on the basis of protection/deprotection and diffusion-limiting strategies, such as using surfactants as a temporary protecting agent to achieve spatial distribution.[14,15] However, limitations exist for these approaches, and a recent study showed that for certain functional species, the use of surfactants as blocking agents may not be very effective to realize spatial selectivity.[16]

We chose a different approach by selecting a composite porous structure that can incorporate single or possibly multiple functionalities. Mesoporous silica spheres were prepared by surfactant templating and used as both a substrate for functional species and a building block for self-assembly, at which stage different functionalities could be introduced separately. We illustrate the procedure for one specific functional group, but in principle, a multifunctional system may be realized by combining a range of differently functionalized "modules". Such modules may even contain mutually incompatible functionalities, if the modules can be kept segregated. In a recent example of a similar concept, porous carbon capsules were loaded with different absorbers and assembled into films by layer-by-layer adhesion.[17] In our approach, the chemically derivatized mesoporous colloids were embedded in another macroscopic porous scaffold through a second templating step, providing a 3D continuous composite porous structure that keeps individual colloids segregated. The use of colloidal spheres and surfactants as cotemplates can lead to materials with controllable pore architectures at two different levels.[18−21] Such hierarchically porous structures were found advantageous as carriers for sensing and catalysis,[22,23] where the hierarchically porous materials outperformed structures with a single pore size in accessibility and diffusion rate.[23] The composite design could prevent the small functional particles from being flushed away and eliminate the need for separation after use.

Herein, we implemented this two-stage fabrication strategy to design composite porous structures as a platform for ion sensing and used a visual response to confirm that embedded probe molecules remained functional and accessible in the prepared membrane. Light is one of the most convenient reporters used in chemical sensing, and direct observation of a color change or spectroscopic monitoring allow for the miniaturization of an analyzer usable in field work. A highly efficient optical system is useful for rapid detection with a minimal analyte volume.[24] Mesoporous silica has been widely explored for ion sensing.[2,25,26] However, chromogenic/fluorescent sensors with mesoporous solids as support were typically prepared in powder form, and the size of particles was still found to hinder the diffusion.[27] Another issue for powders is the difficulty of handling and recycling.[2] Polymers have been used as embedding materials for a mesoporous silica sensor,[28] but they typically produce a composite with low surface area, hydrophilicity, and stability.

The conceptual design is illustrated in Figure 1. Probe molecules capable of responding to the concentration of metal ions are immobilized inside the mesoporous spheres, which are subsequently encapsulated by a poly(methyl methacrylate) (PMMA) layer. The core−shell spheres coassemble with a surfactant-containing silica precursor into a nonclose packed composite structure. After removal of the surfactant and PMMA templates, the resulting material possesses a three-dimensionally ordered macroporous/mesoporous (3DOM/m) structure in which macropores were templated from the core−shell sphere array and mesopores from the surfactant component. In contrast to

(14) Cauda, V.; Schlossbauer, A.; Kecht, J.; Zurner, A.; Bein, T. *J. Am. Chem. Soc.* **2009**, *131*, 11361–11370.
(15) Cheng, K.; Landry, C. C. *J. Am. Chem. Soc.* **2007**, *129*, 9674–9685.
(16) Gartmann, N.; Bruehwiler, D. *Angew. Chem., Int. Ed.* **2009**, *48*, 6354–6356.
(17) Ji, Q.; Yoon, S. B.; Hill, J. P.; Vinu, A.; Yu, J. S.; Ariga, K. *J. Am. Chem. Soc.* **2009**, *131*, 4220–4221.
(18) Yang, P.; Deng, T.; Zhao, D.; Feng, P.; Pine, D.; Chmelka, B. F.; Whitesides, G. M.; Stucky, G. D. *Science* **1998**, *282*, 2244–2247.
(19) Sen, T.; Tiddy, G. J. T.; Casci, J. L.; Anderson, M. W. *Angew. Chem., Int. Ed.* **2003**, *42*, 4649–4653.
(20) Kuang, D.; Brezesinski, T.; Smarsly, B. *J. Am. Chem. Soc.* **2004**, *126*, 10534–10535.
(21) Oh, C. G.; Baek, Y.; Ihm, S. K. *Adv. Mater.* **2005**, *17*, 270–273.
(22) Lebeau, B.; Fowler, C. E.; Mann, S.; Farcet, C.; Charleux, B.; Sanchez, C. *J. Mater. Chem.* **2000**, *10*, 2105–2108.
(23) Chiu, J. J.; Pine, D. J.; Bishop, S. T.; Chmelka, B. F. *J. Catal.* **2004**, *221*, 400–412.
(24) Prasanna de Silva, A. *Nature* **2007**, *445*, 718–719.
(25) Basabe-Desmonts, L.; Reinhoudt, D. N.; Crego-Calama, M. *Chem. Soc. Rev.* **2007**, *36*, 993–1017.
(26) Melde, B. J.; Johnson, B. J.; Charles, P. T. *Sensors* **2008**, *8*, 5202–5228.
(27) Ismail, A. A. *J. Colloid Interface Sci.* **2008**, *317*, 288–297.
(28) Comes, M.; Marcos, M. D.; Martinez-Manez, R.; Sancenon, F.; Villaescusa, L. A.; Graefe, A.; Mohr, G. J. *J. Mater. Chem.* **2008**, *18*, 5815–5823.

previous syntheses involving PMMA spheres and mixed surfactant/silica precursors, the macropores are filled with the functionalized mesoporous silica spheres, forming a 3DOM/m composite with porous discrete spheres (3DOM/m-PODS). In principle, this structure permits multiple parallel functional sites when a mixture of different functionalized spheres is used. In this paper, we detail the assembly and structure of such a composite membrane and demonstrate its function for ion sensing with one type of functional site capable of detecting Cd^{2+} ions.

Experimental Section

Materials. Methanol, methyl methacrylate (MMA), 2,2′-azobis-(2-methyl propionamidine) dihydrochloride (AMPD), cetyltrimethylammonium bromide (CTAB), tetramethyl orthosilicate (TMOS), 3-mercaptopropyl trimethoxysilane (MPTMS), *p*-toluenesulfonic acid (PTSA), 5,10,15,20-tetrakis(1-methyl-4-pyridinio)porphyrin tetra(*p*-toluenesulfonate) (TMPyP), and ethylenediaminetetraacetic acid (EDTA) were purchased from Aldrich. Ethanol and sodium hydroxide were acquired from Mallinckrodt, and cadmium chloride from Baker. Pluronic F127 surfactant ($EO_{106}PO_{70}EO_{106}$) was kindly donated by BASF.

Synthesis. The synthesis of monodisperse mesoporous silica colloids (1 μm) was modified from a protocol by Yano et al.[29] Amounts of 1707 mL methanol, 1050 mL of deionized water, 12 g of CTAB, 6.85 g of NaOH and 3.96 g of TMOS were added into a 3 L Erlenmeyer flask under stirring at 600 rpm. The mixture was stirred for 12 h, followed by another 12 h aging to allow the suspension to sediment. After washing with methanol and drying in vacuo, the white powdery sample was calcined in air flow at 550 °C for 6 h to remove organic species and then sonicated in a water/ethanol mixture (50/50 wt %) for 12 h to regenerate surface hydroxyl groups.

To chemically immobilize chromophores in the mesoporous silica colloids, we first grafted MPTMS onto the pore surface by refluxing ca. 2 g of silica colloids with 2 g of MPTMS and 0.05 g of PTSA as catalyst in 50 mL of toluene for 12 h. After being washed and dried, the MPTMS-grafted sample was dispersed in 5% H_2O_2 solution and stirred for 24 h at 50 °C to convert mercapto groups to sulfonate groups. The immobilization of TMPyP was performed by mixing the sulfonate-terminated silica with ca. 2 mg dye in 50 mL H_2O, sonicating for 2 h, drying in vacuo, and washing repeatedly with H_2O.

Dye-containing silica/PMMA core−shell colloids were synthesized by modifying a standard emulsion polymerization of MMA.[30] A volume of 10 mL of a dye-containing silica colloid dispersion (ca. 10 wt % solid content) was added into a 1 L flask containing 600 mL H_2O and heated to 70 °C on an orbital shaker at 100 rpm under nitrogen protection, followed by the addition of 0.2 g of AMPD as the initiator. After the temperature was stabilized, 12 g of MMA was quickly poured into the flask and the cap was replaced immediately to minimize air exposure. The polymerization reaction was allowed to proceed for 1 h. The desired core−shell particles were then isolated from the emulsion via centrifugation at 1500 rpm and washed three times with H_2O.

After centrifugation, the core−shell particles were redispersed as a ca. 50 wt % dispersion in water. Meanwhile, a silica precursor was prepared by mixing TEOS, HCl (37%) and F127 with a weight ratio of 5:2:4 and stirring until the mixture was uniform. Then the particle dispersion and silica precursor were mixed in 1:1 weight ratio and stirred for 2 h until the dispersion became homogeneous. The resulting material was a viscous but flowable dispersion that could be stored in a capped vial for several days.

To cast a hierarchically porous film, we spin-coated the precursor onto a silicon wafer substrate with a homemade spin coater[31] using a spinning rate close to 1000 rpm for 1 h. The as-synthesized film was stored at 50 °C for 24 h, and afterward, the polymer templates were extracted by soaking in toluene at 50 °C for 12 h.

The Cd^{2+} solutions were prepared by dissolving appropriate amounts of $CdCl_2$ in H_2O to reach the desired concentrations (5, 20, and 100 ppb) and adjusting the pH of the solutions to 9.5 with 1 M NaOH. To confirm access to the trapped dye molecules by visual inspection of the ion recognition process, the film of 3DOM/m-PODS supported on a glass substrate was directly soaked in these solutions. For UV−vis measurements, a small piece of the film of 3DOM/m-PODS was detached from the substrate and placed into a quartz cuvette filled with Cd^{2+} solution.

Characterization. Scanning electron microscopy (SEM) images were taken using a JEOL 6700 field emission microscope at an accelerating voltage of 5 kV. Samples were not metal-coated for SEM analsis. Transmission electron microscopy (TEM) images were recorded on a FEI Tecnai 12 microscope with a LaB_6 filament working at 120 kV. Samples were dispersed in ethanol for 30 min with sonication and then deposited onto a Lacey-Formvar/carbon-film-coated copper grid. Small-angle X-ray scattering (SAXS) patterns were acquired on a Siemens D5005 X-ray diffractometer. Nitrogen adsorption/desorption measurements were performed on a Quantachrome Autosorb-1 gas sorptometer. Thermogravimetric analysis (TGA) was performed on a Netzsch STA 409 analyzer. Samples were heated under air flow from room temperature to 1000 at 5 °C/min. Zeta potential measurements were taken on a Brookhaven Instruments ZetaPlus analyzer. UV−vis spectra were taken on a Hewlett-Packard 8452A diode array spectrophotometer in transmission mode.

Results and Discussion

Mesoporous Silica for Ion Sensing. Mesoporous silica materials are suitable carriers for various functional species because of their large surface areas, their chemical inertness/biocompatibility and their capability for diverse surface functionalization. Mesoporous silica spheres, uniformly sized around 1 μm and possessing controlled mesopore architecture provide additional advantages such as rapid mass diffusion to active sites and easy integration with other structures and systems.[29] Here, monodisperse silica spheres featuring radially oriented, 2D hexagonal mesopores were used as the solid support for a well-established Cd^{2+} chromophore. The mesopores contained grafted sulfonate surface groups, which were subsequently used for the immobilization of ion-selective probe molecules. As a proof of concept, we chose TMPyP probe molecules as selective metal ion detectors, which

(29) Yano, K.; Fukushima, Y. *J. Mater. Chem.* **2004**, *14*, 1579–1584.
(30) Schroden, R. C.; Al-Daous, M.; Sokolov, S.; Melde, B. J.; Lytle, J. C.; Stein, A.; Carbajo, M. C.; Fernandez, J. T.; Rodriguez, E. E. *J. Mater. Chem.* **2002**, *12*, 3261–3267.
(31) Chakraborty, M.; Chowdhury, D.; Chattopadhyay, A. *J. Chem. Educ.* **2003**, *80*, 806–809.

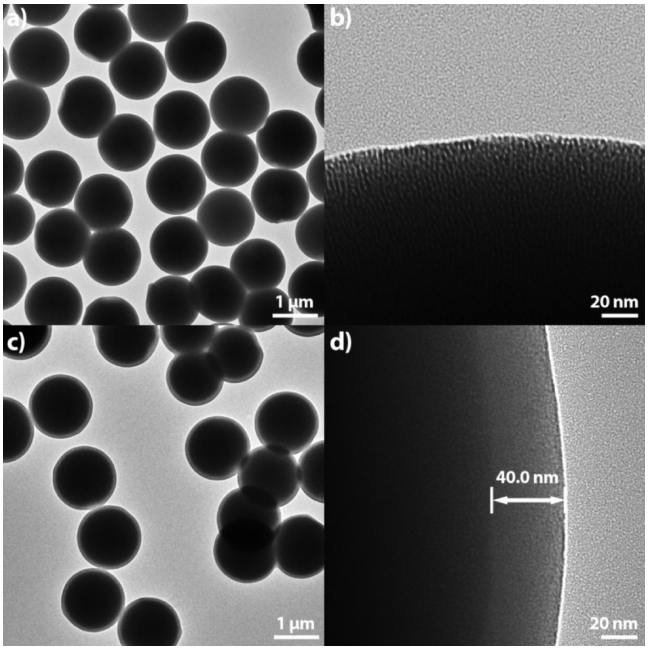

Figure 2. TEM images showing (a) the dye-containing mesoporous silica spheres; (b) a zoomed-in view revealing mesopores; (c) core−shell particles; (d) a detailed view of the PMMA shell structure.

have previously been demonstrated to selectively bind with Cd^{2+} ions.[32,33]

Mesoporous Silica Spheres with TMPyP. The as-synthesized mesoporous colloidal silica spheres were characterized using TEM. As shown in Figure 2a, the size of the silica colloids was uniform with an average diameter of 1.30 ± 0.03 μm. The large sphere size was chosen here because smaller spheres (300−600 nm), when forming arrays, showed strong photonic effects in the visible range and may interfere with optical sensing. The radial orientation of the hexagonal mesopores was observed along the edge of the spheres in the zoomed-in image (Figure 2b). The mesopore structure of the silica spheres was further characterized with SAXS and N_2 adsorption (see later discussion and Figure 8). The SAXS pattern confirmed the presence of 2D hexagonal mesophase with a d_{100}-spacing of 2.96 nm, and the adsorption analysis showed that the sample had a BET surface area of 1326.8 m^2/g and a pore size centered at 1.80 nm. The mesoporous silica spheres were then grafted with MPTMS and the propylthiol groups were oxidized to sulfonate groups[3] for the immobilization of probe molecules through electrostatic attraction (Figure 3).

Encapsulation in PMMA. The dye-containing mesoporous silica colloids were subsequently encapsulated in PMMA. Previously, mesoporous silica/polymer shell colloids were mainly synthesized through a grafting-from strategy, namely with covalently bonded surface species to induce surface polymerization.[34] In the current study, because the PMMA protective layer needs to be removed

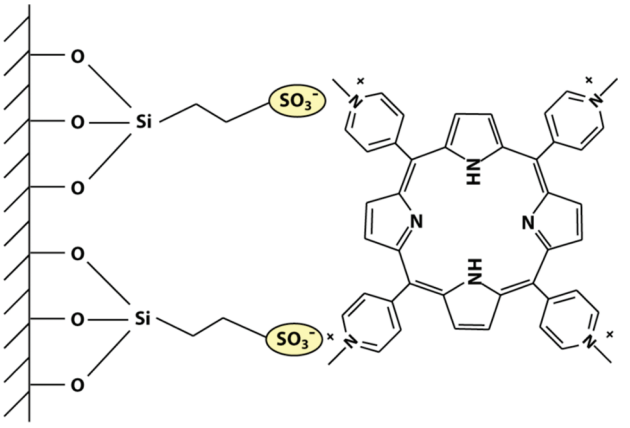

Figure 3. Schematic illustration of immobilized TMPyP on sulfonate-functionalized silica mesopore walls.

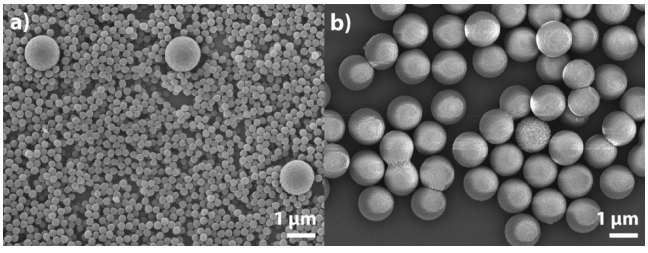

Figure 4. (a) SEM image of as-synthesized SiO_2−PMMA core−shell colloids together with much smaller primary PMMA particles. (b) Purified core−shell colloids after centrifugation.

in the following step, no chemical anchors were supplied on the external surface of the silica spheres and no cross-linker was added. Therefore, the SiO_2−PMMA core−shell colloids were formed through in situ polymerization in an adapted emulsion polymerization process, where coating with PMMA was facilitated by electrostatic attraction. This method produced a mixture of PMMA surface-coated silica spheres and smaller primary PMMA spheres. The latter, however, could be readily removed through centrifugation (Figure 4). As the probe-containing spheres were negatively charged (see below for zeta-potential results), the cationic initiator AMPD was employed to induce the surface coating of PMMA on the silica colloids. The PMMA thickness in this work was estimated to be ca. 40 nm by TEM. Because it is critical to preserve the activity of the dye during the polymer encapsulation, the synthesis conditions were investigated for their potential influence on the dye activities. It was found that the dye activities could be preserved, unless the polymerization was conducted above 80 °C, at which temperature a reaction between porphyrin and MMA might be possible.[35]

To evaluate the effectiveness of the grafting and encapsulation processes, zeta-potential measurements were performed following these procedures (Figure 5). The initial mesoporous SiO_2 spheres showed slightly negative potentials at pH 7, corresponding to partially deprotonated silanol groups. After TMMPS grafting and oxidation,

(32) Balaji, T.; El-Safty, S. A.; Matsunaga, H.; Hanaoka, T.; Mizukami, F. *Angew. Chem., Int. Ed.* **2006**, *45*, 7202–7208.
(33) El-Safty, S. A.; Prabhakaran, D.; Ismail, A. A.; Matsunaga, H.; Mizukami, F. *Adv. Func. Mater.* **2007**, *17*, 3731–3745.
(34) Radu, D. R.; Lai, C. Y.; Wiench, J. W.; Pruski, M.; Lin, V. S. Y. *J. Am. Chem. Soc.* **2004**, *126*, 1640–1641.
(35) Smith, K. M. *The Porphyrin Handbook*; Academic Press: New York, 1999.

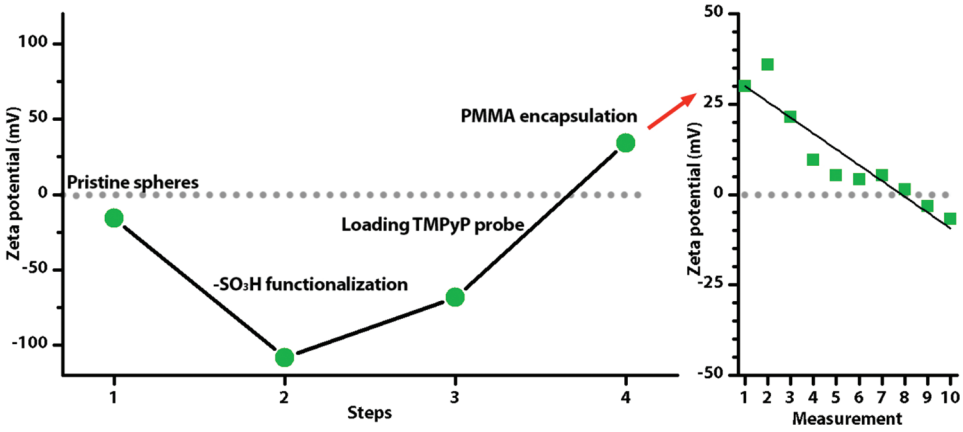

Figure 5. Left: Zeta potentials of the colloidal particles during different stages of the synthesis. Right: Plot showing the zeta-potential change during 10 consecutive measurements for SiO_2−PMMA core−shell colloids.

the zeta-potential decreased dramatically to −110 mV, indicating the pore surface was now populated with strongly acidic sulfonic acid groups that formed negatively charged sulfonate groups upon deprotonation. Once the surface was tethered with TMPyP, the surface charge was partially neutralized and the potential became less negative (−70 mV). Finally, after PMMA encapsulation, charge inversion occurred on the colloidal surface because of the cationic initiator. Interestingly, after multiple measurements, the surface charge of the core−shell particles declined and eventually returned to a negative value again. This may indicate that the PMMA layer had low adhesion with the underlying silica surface and therefore could be stripped off during electrophoretic motion.

Composition of the Core−Shell Spheres. The extent of surface functionalization and PMMA encapsulation was also characterized using TGA (Figure 6). From the thermogravimetric results in combination with N_2 adsorption data, the density of surface hydroxyl groups was estimated to be 1.2/nm^2.[36] Assuming that grafting TMMPS did not significantly change the number of surface silanols (because of incomplete condensation), the surface density of propylthiol groups was calculated to be 0.6/nm^2. The actual density of sulfonate groups, after oxidation, became lower due to partial cleavage during oxidation.[3] The amount of TMPyP was 2.8 wt % of the original silica spheres. After encapsulation, the weight of the PMMA coating was 59.4% of the original silica spheres. Toluene extraction proved to be only moderately effective, and 54.0% PMMA could be removed through this process. Further improvement of the extraction efficiency may require optimization of the PMMA polymerization, or resorting to other techniques such as using cleavable cross-linkers. Nevertheless, the probe molecules were shown to be still active and easily accessible, and the spheres gave color responses that were virtually indistinguishable from those of the original spheres.

Coating with PMMA is an important step for the following composite formation process. The PMMA capsule protected the mesoporous silica spheres from being exposed to the silica precursor in the subsequent assembly step, which could have blocked the mesopores and/or reacted with the surface functional species. For example, direct mixing of silica spheres with the silicate precursor caused a rapid sol−gel reaction and led to instant precipitation because of the surface hydroxyl groups and acidic entities.

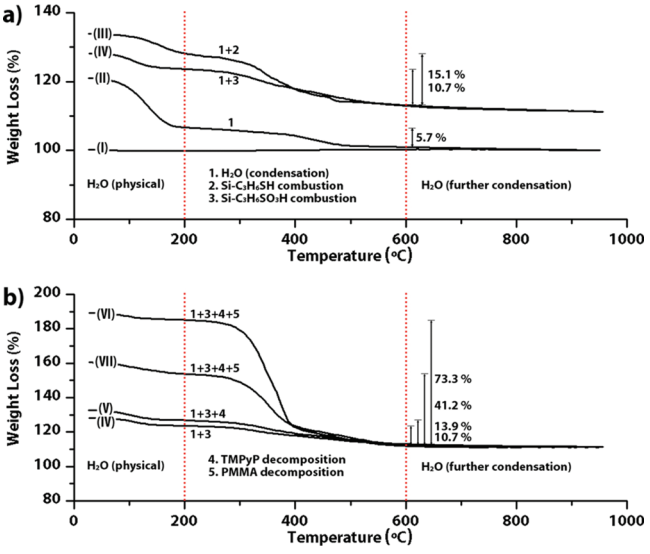

Figure 6. Thermogravimetric analysis of TMPyP-loaded SiO_2−PMMA core−shell particles during different stages of the synthesis. The percentage weight loss was rescaled on the basis of the weight of pristine SiO_2 spheres after calcination. This allows for direct comparison between different samples. Processes causing weight loss between 200 and 600 °C are labeled in the figure. Curve assignment: (I) as-calcined SiO_2 mesoporous spheres, (II) SiO_2 after rehydroxylation, (III) MPTMS-grafted SiO_2, (IV) sulfonate-terminated SiO_2 after oxidation, (V) TMPyP-loaded SiO_2, (VI) TMPyP-loaded SiO_2−PMMA core−shell spheres, (VII) core−shell spheres after toluene extraction.

Structure of the Composite Film. The isolated silica/PMMA core−shell particles were then redispersed into an aqueous mixture of silica precursor, surfactant and HCl, forming a dispersion that contained ca. 25% composite colloids in a liquid-crystal-like silicate-surfactant phase. The dispersion may be processed into thin films through spin coating or drop casting. Here, a spin-coating technique was adopted, as it was capable of producing a uniform, nonclose packed sphere array in

(36) Zhao, X. S.; Lu, G. Q.; Whittaker, A. K.; Millar, G. J.; Zhu, H. Y. *J. Phys. Chem. B* **1997**, *101*, 6525–6531.

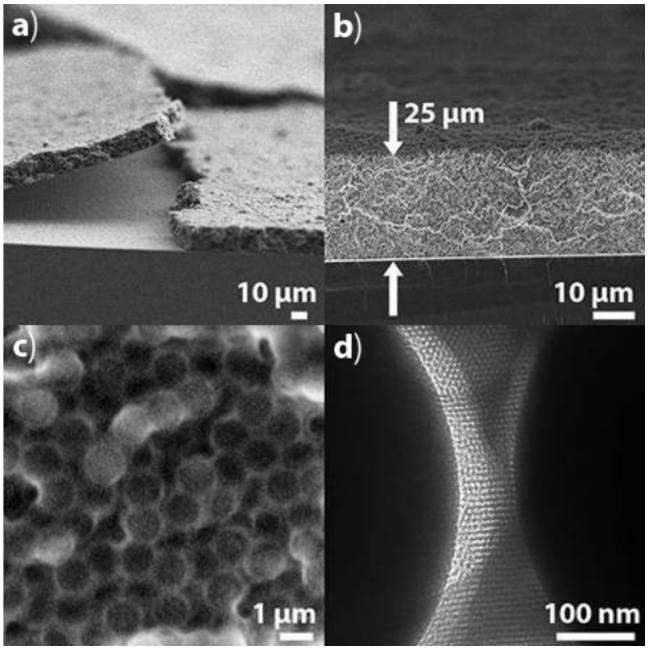

Figure 7. (a) SEM image showing an overview of the composite film. (b) Cross-sectional view of the composite film. (c) SEM image showing the composite structure of spheres within the 3DOM/m silica matrix. (d) TEM image revealing the mesoporous structure in the silica matrix used to embed the spheres.

a liquid medium.[37] After solvent extraction to remove the surfactant and the polymer shell, a hierarchically porous composite film, i.e., a 3DOM/m-PODS film bearing active functionalities was obtained. The spin-coated thin film was soft, smooth and even elastic in the solvent and could be handled easily. Images a and b in Figure 7 show the overview of the film, which was measured to have a thickness of 25 μm. Figure 7c shows a SEM micrograph of the composite thin film, in which the core−shell colloids were embedded in the silicate matrix. The silica spheres were all approximately equally spaced with short-range packing order. The mesoporous silica spheres were not in direct contact, instead they were separated by a mesoporous silica matrix. Figure 7d shows that the silica matrix possessed an ordered hexagonal mesoporous structure templated from the F127 surfactant. The mesopores connected the functional spheres within each individual macropore and therefore permitted easy access by an analyte-containing fluid.

Dual mesoporosity of the 3DOM/m-PODS materials was further characterized by SAXS and N_2 adsorption (Figure 8). Because template removal was incomplete during the mild solvent extraction process, the sample was calcined in air at 600 °C for 6 h to remove all the organic species and allow us to unambiguously determine the mesostructures. Because CTAB and F127 are surfactants of very different sizes, the resulting mesoporous structures also possess different *d*-spacings (Figure 8a). The SAXS pattern of the 3DOM/m-PODS sample clearly showed two primary peaks (Figure 8b). The first peak corresponding to a d_{100}-spacing of 2.81 nm resulted from scattering by the hexagonal mesophase in the spheres. The small decrease in *d*-spacing compared to the non-embedded mesoporous silica spheres was likely due to shrinkage during the second calcination step. The peak at 9.81 nm, when compared with a control sample templated with pure PMMA spheres (Figure 8a), was assigned to a mesophase from the surrounding silica matrix. The apparently stronger diffraction from the mesoporous matrix compared to that of the mesospheres was due to the fact that the framework had a more three-dimensionally continuous structure, i.e., larger domains, than the radially oriented hexagonal mesopores in the individual spheres,[29] although background scattering also contributed to this effect. The dual mesoporosity was also confirmed by the N_2 adsorption measurements, which displayed two-stage hysteresis loops (Figure 8c), and the BJH pore size distribution clearly showed the existence of two different sizes of mesopores (Figure 8d). Because the silica colloids possessed smaller mesopores than the mesoporous matrix, the sequential adsorption/desorption steps from the two contributors did not interfere with each other. Also, N_2 uptake near unit relative pressure was observed, corresponding to condensation in textural pores, i.e., the spaces between the colloidal spheres and the matrix. Note that the adsorption in this region was much less pronounced than in previous 3DOM/m silica samples with interconnected macropores,[9,38] because once the mesopores were filled by condensed N_2, the N_2 would have virtually no access to the inside of the macropores, in contrast to previously described 3DOM/m silica samples where access was maintained through macropore windows.[9] This further confirmed that the macropores in the current structure were mostly noninterconnected.

Cd^{2+} Ion Detection with 3DOM/m-PODS. To demonstrate that the organic TMPyP probe molecules incorporated in the mesoporous silica spheres remained intact after all the processing steps to produce the 3DOM/m-PODS films (including extraction of PMMA but no calcination), and to show that they remained accessible to analytes, we tested the films for Cd^{2+} detection. Previously, it was demonstrated that TMPyP incorporated in mesoporous silica is highly sensitive and selective for Cd^{2+} ions within a given pH range, allowing for visual inspection of the sample by color changes.[32,33] Following the published protocol, the pH of the Cd^{2+} solutions was set at a value of 9.5.[33] We found that the response of the dyes to Cd^{2+} ions within the mesoporous silica spheres in the 3DOM/m-PODS structure was effectively preserved, and the incurred color change could be easily identified by eye when Cd^{2+} ions were present (Figure 9, insets). This observation indicates that the activity of the probe molecules was not compromised despite the fact that multiple manipulations, including PMMA encapsulation, sol−gel reaction, and solvent extraction, were performed after the probe molecules were grafted. The adsorbed Cd^{2+} could be readily removed by using EDTA as a stripping agent,

(37) Jiang, P.; McFarland, M. J. *J. Am. Chem. Soc.* **2004**, *126*, 13778–13786.

(38) Sen, T.; Tiddy, G. J. T.; Casci, J. L.; Anderson, M. W. *Chem. Mater.* **2004**, *16*, 2044–2054.

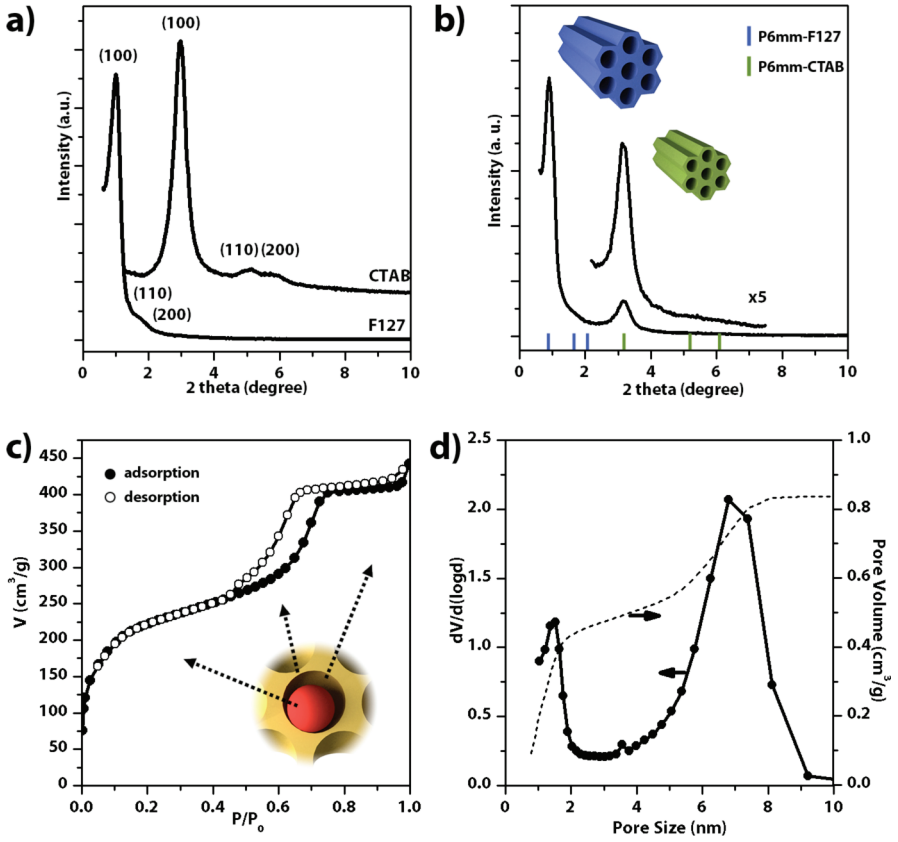

Figure 8. SAXS and N_2 sorption data. (a) SAXS patterns of mesoporous silica spheres (templated by CTAB) and a control 3DOM/m matrix synthesized with PMMA spheres (templated by F127). (b) SAXS pattern of the 3DOM/m-PODS. (c) N_2 adsorption/desorption isotherm of the calcined 3DOM/m-PODS. (d) BJH pore size distribution and cumulative pore volume of 3DOM/m-PODS.

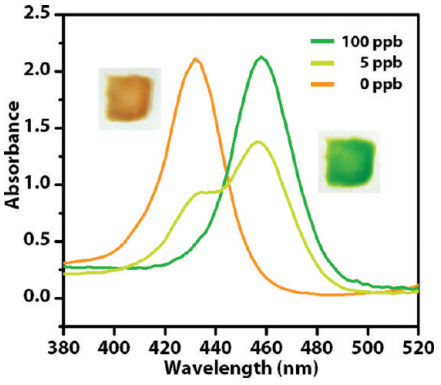

Figure 9. UV−vis absorption spectra of 3DOM/m-PODS sensing membranes exposed to solutions containing the indicated concentrations of Cd^{2+} ions. The insets show digital photographs of the sensing membrane as synthesized (left) and in 20 ppb Cd^{2+} solution (right).

and the regenerated membrane may therefore be used again, although with slower response, in line with a previous report.[33] The robustness of the film was satisfactory, and no visible cracks were observed in the film after it was cycled between different solutions. The response of the composite film was also quantitatively examined by UV−vis absorption spectroscopy (Figure 9). In the absence of Cd^{2+}, the TMPyP molecules produced an adsorption peak at ca. 435 nm. With 5 ppb Cd^{2+}, an additional peak at ca. 460 nm was detected and the intensity of the original adsorption at 435 nm decreased. The adsorption at 435 nm disappeared completely in the presence of 100 ppb Cd^{2+}, corresponding to the complete color change of the sample. Because the UV−vis spectra were taken in transmission mode, these observations confirmed that the TMPyP molecules in the internal mesopores of the film were fully accessible and could form complexes with incoming Cd^{2+} ions.

Conclusions

We described the fabrication of composite porous structures consisting of noncontacting mesoporous spheres embedded in a hierarchically porous matrix, which stabilized the spheres while keeping internal mesopores accessible to external fluids. In this facile method, mesoporous silica spheres were utilized as functionality carriers, whereas the overall scaffold was constructed via a secondary colloidal crystal/surfactant templating process. This two-stage approach combined with the benign synthetic environment allows one, in principle, to prepare multiple sets of mesoporous spheres with different functional groups ("modules"). Especially because the porous matrix keeps the components separated after film casting, the coexistence of multiple, incompatible functional species within a composite structure should be possible. To demonstrate that those steps can indeed preserve and allow access to the internal functional species in the matrix, we incorporated an ion-sensing component into mesoporous silica spheres as a proof of concept and created a 3DOM/m-PODS membrane capable of Cd^{2+}

detection. The possibility of including multiple probes in similar structures will be examined in ongoing work.

Acknowledgment. This work was financially supported by the National Science Foundation (DMR-0704312). Parts of this work were carried out in the University of Minnesota Characterization Facility, which receives partial support from the NSF through the MRSEC, ERC, MRI, and NNIN programs. The authors thank Dr. Wei Fan for the N_2 adsorption measurement.